Joint EPRI – 123HiMAT International Conference on
Advances in High Temperature Materials
October 21–24, 2019, Nagasaki, Japan
J. Shingledecker, M. Takeyama, editors
https://doi.org/10.31339/asm.cp.am-epri-2019p0035

IN SITU MEASUREMENT OF PARTICULATE EROSION DAMAGE ON ADDITIVELY MANUFACTURED IN718

A.T.Fry, J.Nunn, M.G.Gee, L.Orkney
National Physical Laboratory, Teddington, Middlesex, UK

ABSTRACT

The measurement of damage from high temperature solid particle erosion (HTSPE) can be a lengthy process within the laboratory with many lab-based systems requiring sequential heat and cooling of the test piece to enable mass and/or scar volume measurements to be made *ex situ*. Over the last few years a new lab-based system has been in development at the National Physical Laboratory which has the ability to measure the mass and volume change of eroded samples *in situ* without the need to cool the sample. Results have previously been shown demonstrating the *in situ* mass measurement, more recently the *in situ* volume measurement capability has been added and used to evaluate the erosion performance of additively manufactured materials.

Selective laser melting (SLM) is an advanced manufacturing method which is growing in popularity and application. It offers the ability to manufacture low volume complex parts and has been used in rapid prototyping. As the technique has developed there is increasing interest to take advantage of the ability to manufacture complex parts in one piece, which in some case can be more cost and time effective than traditional manufacturing routes. For all the benefits of SLM there are some constraints on the process, these include porosity and defects in the materials such as 'kissing bonds', surface roughness, trapped powder and microstructural variation. These features of the processing route may have implications for component performance such as strength, fatigue resistance wear and erosion. To investigate this further SLM IN718 has been used to evaluate factors such as surface roughness, microstructure and morphology on the erosion performance as measured *in situ* and compared with conventional produced wrought IN718 material.

INTRODUCTION

Shortened service life of mechanical components, such as rotating parts, and other complications due to wear are a considerable financial and time burden for the power generation and aerospace industry. Guides have been published to help engineers assess the damage and manage the consequent degradation of plant and equipment [1], but erosion is still a significant problem. Erosion differs from wear in that it does not involve the repeated interaction of two separate surfaces coming into repeated contact. In the case of erosion there is material loss from discrete impact with multiple surfaces, principally solid particles such as grit, oxide water etc. Irrespective of the initial cause of the damage the resulting mechanical and financial consequences may be similar.

The accumulation of damage will ultimately impact the efficiency of the plant, increasing emissions and running costs. Mitigation against high temperature solid particle erosion (HTSPE) can be achieved through surface engineering approaches of modifying the surface of the component through processes such as shot peening, and by applying a coating to the surface to act as an erosion barrier. Advanced manufacturing techniques such as selective laser melting (SLM), electron beam melting (EBM), wire additive manufacturing (WAM) etc. provide the opportunity to build a graded microstructure and thus tailor the properties of the surface to meet different requirements. The application of additive manufacturing to rapid prototyping of engineered surfaces can be used to develop erosion resistant surfaces, for example blading in turbines, and so accelerate the introduction of improved materials into industrial applications.

To facilitate the development and validation of new material solutions test methods and test equipment should be as efficient as possible. In the last few years a new ASTM [2] test standard has been published. In addition, a new HTSPE test system has been in development at NPL. Initially as part of the EURAMET METROSION [3] project this test facility was designed and constructed with the aim to produce a versatile apparatus with embedded instrumentation to monitor and control the temperature of the gas, sample and particles, to measure and control the gas velocity [4] and to measure the mass change [5] and erosion scar volume in-situ during the test. This facility can vary the impact angle, gas/particle velocity, temperature and stand-off distance from the sample. This helps to provide a better understanding of the influence of the apparatus features, such as the ratio of the acceleration length to nozzle diameter and the stand-off distance of the nozzle from the sample as a function of temperature and velocity. Work has been previously reported describing a comparison of HTSPE data for Nimonic

80A [5] which focussed on the influence of the apparatus design and the test method on the erosion measurements [6]. This work demonstrated the use of *in situ* mass measurement to determine the erosion rate, comparing these *in situ* measurements with *ex situ* measurements conducted by project partners, an example of the results is shown in Figure 1.

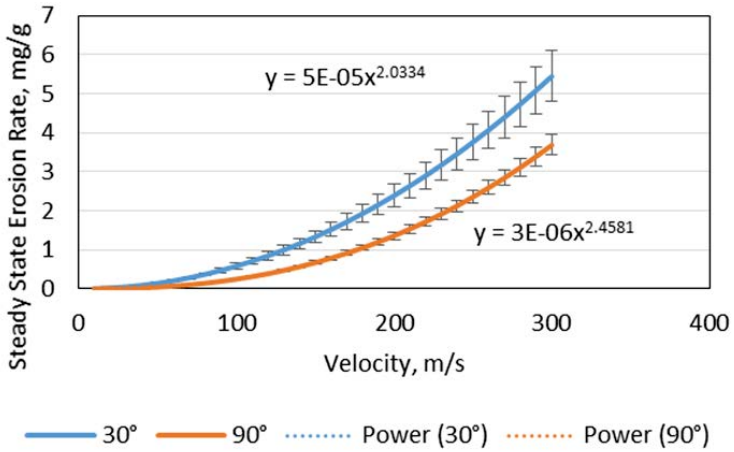

Figure 1 Erosion rate as a function of incident angle for all data collected by project partners for Nimonic 80A at 600 °C [6].

In conjunction with *in situ* mass measurement a method to measure the volume of material removal *in situ* during the erosion test has also been in development. Until very recently the method developed had only been demonstrated at room temperature and *ex situ* on the bench top [7]. The work presented in the following paper reviews the approach used and demonstrates the results of *in situ* measurements, a comparison is presented of wrought IN718 material to SLM IN718 material.

MEASUREMENT PRINCIPLE

The *in situ* volume scanner developed in this work uses a line laser and a conventional digital SLR camera, using the principle of laser triangulation [8]. Commercial systems are available for these measurements, but none of the available systems had the combination of violet light and large measurement stand-off distance, both required to enable easements to be made at elevated temperature.

For this application, it is important that surface is optically rough so that it does not produce a specular reflection but a diffuse one, this is not normally an issue with this form of test as the surfaces are usually as machined ground flat, but not polished. Although this may give rise to speckle [8] it makes it possible for the camera to image the position of the projected line on the surface without being saturated by an intense specular reflection. Ultimately what matters for the measurements is the position where the line laser illuminates the surface and not the direction in which the combination of blue light subsequently reflects.

When a line laser is projected perpendicularly on to a surface, the line will appear like a straight line when viewed from the same direction as the line laser source. This will be true whether the surface is flat or curved. However, if the line laser is made to shine on a surface at an angle that is significantly different from the observation angle, the line will only appear straight if the surface is perfectly flat. If the surface of the specimen has bumps or dents the laser line will appear distorted. The sensitivity of the projected line deflection to the height or depth of the surface feature is higher if the glancing angle of the laser illumination (A) is made smaller, see Figure 2. Although a smaller illumination angle would increase the sensitivity, it would make it impossible to illuminate erosion scars with steep edges.

To enhance the sensitivity of the arrangement, the camera is placed on the opposite side of the sample from the laser. Ideally the camera would be placed perpendicularly above the plane of the surface, but this position is not

available as it is needed for the erodent injection system. A compromise was reached whereby both the line laser and the camera are mounted at 45 degrees to the surface of the specimen (A =B=45 degrees in Figure 2. The angles A and B are also shown in Figure 3).

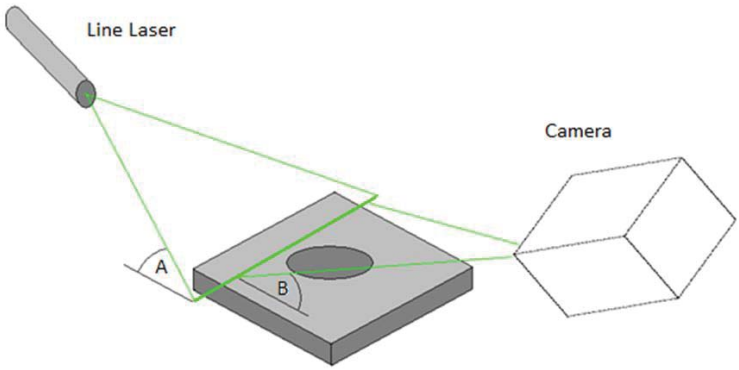

Figure 2 Schematic illustrating the principle of the erosion scar measurement technique.

A change in surface height affects where the scattered light is seen to be coming from, as shown in Figure 3. It should be noted that of all the light scattered from the surface of the scar, only the light scattered in the direction of the camera (marked with arrows towards the camera) will be collected to form the image.

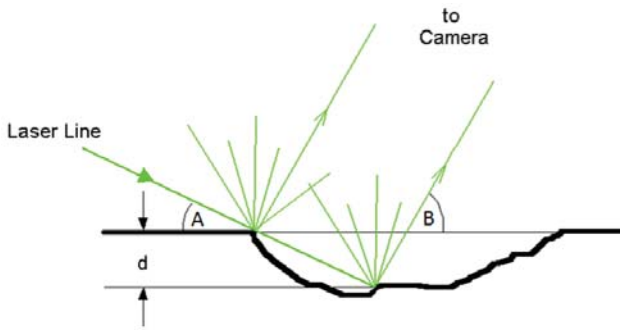

Figure 3 Detail of how a change in vertical surface height affects the position at which the line laser will strike the surface, and hence where the scattered light will originate from.

Figure 4 shows the left-hand side of the erosion scar shown in Figure 3. The laser line illumination comes towards the surface originating at the top left-hand side making an angle A with the flat surface of the sample. The ray that grazes the undamaged surface proceeds to strike inside the erosion scar at a depth d below the original surface and there the light is scattered towards the camera, making an angle C between the incident ray and the scattered ray as shown in Figure 4. L is the lateral displacement along the original surface of the sample between where the incident ray first strikes the still undamaged surface and the place from which the scattered ray goes past that surface line on the way towards the camera.

Using basic trigonometry, we find the following relationships:

A+B+C =180° (true for all triangles), therefore	C =180°-A-B	(eq. 1)
(Sin C)/L = (Sin B)/X (Sine rule), therefore	X = L (Sin B)/(Sin C)	(eq. 2)
Sin A = d/X, therefore	d = X Sin A	(eq. 3)
Combining equations 1, 2 and 3,	d = L [Sin A Sin B]/[Sin (180-A-B)]	(eq.4)

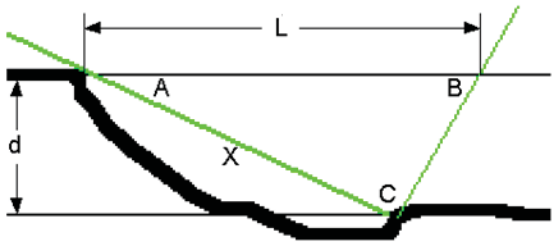

Figure 4 Schematic diagram used to derive the theory.

Note:

A – The length L is the actual distance along the surface from which the laser scatters with respect to the undamaged surface. Since the camera is not observing from directly overhead, the camera will measure L obliquely and therefore the value of L that is obtained must be corrected for this.

B – Since the camera is imaging the surface obliquely the image magnification will be different in X and Y directions. (Oblique Magnification = Magnification x (Sin B)).

To obtain the best measurement capability, it was necessary to ensure adequate resolution both in terms of pixel count as well as optical resolving power of the lens. To achieve this a Canon EOS 600D with an f100 to f300 Zoom lens was used which consisted of; an image sensor size 22.3 x 14.9 mm with 5184 x 3456 pixels (~18 Mpixel), pixel size 4.3 um, Zoom lens 75-300 mm. A bellows is used to make it possible for the zoom to focus on an object that is only 45 cm away from the camera. Because the camera is being used in a "Macro" configuration, the depth of focus becomes an issue when using the full aperture of the lens. It was necessary to reach a compromise between resolution and depth of focus, by stopping the lens aperture down to f16. This means that to get adequate image intensity the shutter is being operated at around 0.25 s. However, since the camera is mounted rigidly on to the system this did not pose any problems. Prior to obtaining images it is important to calibrate the magnification of the system. This was achieved by means of a dimensional transfer standard. The grid shown in Figure 5 was first measured with a travelling microscope in the X and the Y directions. The transfer standard was then imaged with the camera mounted at approximately 45 degrees. Careful measurements of the image taken at an oblique angle made it possible to calculate the X and Y magnifications separately, and from their ratio the angle of the camera was found to be 49 degrees.

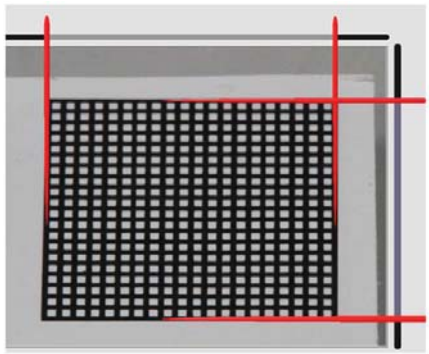

Figure 5 Transfer dimensional standard used to calculate camera magnification and angle.

Each image obtained by the camera only provides a single depth profile across the surface of the specimen; to obtain a full surface map it is necessary to move the laser line (maintaining the same angle A) so that it is projecting

on to a new part of the specimen. Many separate images need to be obtained, starting with the laser line on the surface where no wear has occurred and gradually moving through the scar until the laser line reaches the bottom of the surface where, again, there is no wear. These two unworn surfaces provide the datum reference levels. Once a series of images have been captured a LabVIEW programme is used to perform the image analysis, this process has been previously described [7]. After the image has been analysed a single profile is outputted for each image, these profiles are combined to produce a depth map, Figure 6.

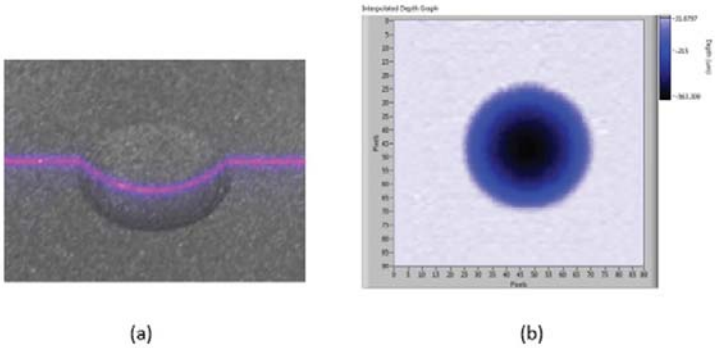

Figure 6 (a) Typical image obtained on the reference dimple depth standard, (b) depth map obtained with a laser line spacing of 1/8th mm. The dimple diameter is approximately 4.7 mm.

Bench top validation of the process was conducted using an aluminium reference sample which had dimples machined into it, and on aluminium samples which had been eroded, a full description of these tests is discussed in [7]. To summarise, the measurements showed that *ex situ* the measurement system had good agreement with other optical microscope measurement systems, such as the Alicona 3D optical microscope, of less than 4%, with the level of agreement in depth measurement being is typically ±10 µm. Figure 7 shows a typical Alicona height map and profile on the left-hand side, and corresponding Laser Line results on the right-hand side.

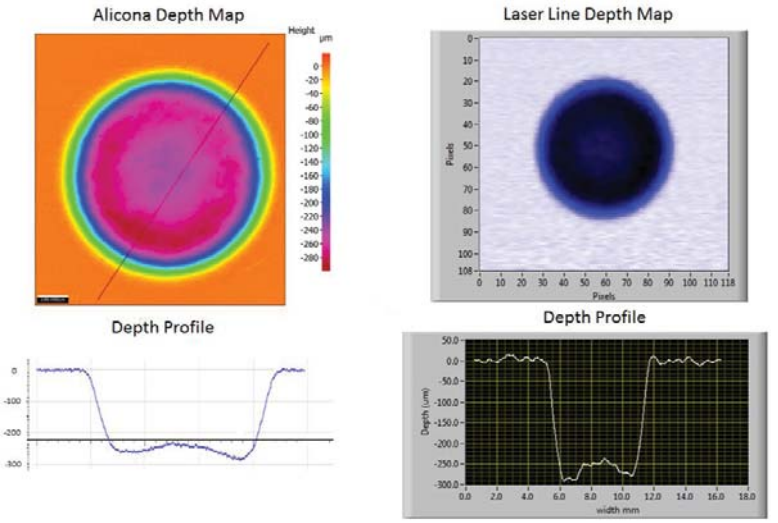

Figure 7 Typical results on the nominally 0.3mm specimen: Alicona 3D Optical Microscope (left) and Laser Line Method (right).

EXPERIMENTAL METHOD

The HTSPE tests were conducted using the modified NPL HTSPE apparatus, shown in Figure 8. Originally the apparatus used a furnace to maintain the sample at the test temperature. Whilst this was found to work, the furnace lining did experience issues of erosion itself and the furnace did obstruct line of sight for the laser optics. Consequently, the apparatus was modified to incorporate an induction heater which surrounds the sample. The induction coils are protected from damage using a ceramic sheath as shown in Figure 8. All other features of the original design [5] remain unchanged with the rig consisting of an air pump which delivers air at a flow rate of $400 m^3 h^{-1}$ (235 $cuft.min^{-1}$), which is delivered at a pressure of 1 bar. The air passes through a heater cartridge located under the nozzle, where it is heated to the test temperature, with an upper limit of 900 °C. The hot gas then passes through the nozzle where a reduction in cross section occurs, thereby accelerating the gas further. The velocity of the gas is governed by the flow rate from the air pump. The erodent powder is introduced into the gas stream after the 'throat' [4] section of the nozzle, where it accelerates along the nozzle length (200 mm) before exiting and impinging on the specimen surface, in this case at 90° to the flow direction. The stand-off distance between the sample and the nozzle can be varied, for the work presented here it was set to 40 mm.

Figure 8 Internal view of the HTSPE apparatus showing the induction heater, sample hang down and laser optics.

Measurements have been performed at room temperature and at 400 °C and 500 °C. In the case of the elevated temperature tests the sample is heated to the required temperature using the induction heater. The gas is heated to a temperature greater than the test temperature to allow for adiabatic expansion of the gas on exit from the nozzle which leads to a drop in the gas temperature. In all cases the erodent used was Saftigrit White, which is a 230-mesh alumina powder. The velocity of the erodent can be directly measured using the image velocimetry system developed in METROSION [9]. This provides a velocity distribution plot for a statistically meaningful number of particles within the size distribution, an example of this is shown in Figure 9 for measurements at 700 °C. For the elevated temperature tests the gas was heated to a temperature of 500 °C and 600 °C respectively, this produced a mean particle velocity of 225 ms^{-1}. The HTSPE tests were conducted using an impact angle of 90° with erodent aliquots of 5g, controlled by a commercial powder feeder. After each aliquot of erodent, the surface of the sample was scanned to measure the volume of the scar. At the end of each test the sample was weighed, and the volume of material removal calculated based on the density of the samples.

Two batches of IN718 material were eroded, the first was commercial grade IN718 which had been forged, solution annealed, age hardened and peeled. The chemical composition is shown in Table 1. Hardness measurements according to ASTM E18-18a had been performed on the material and average HRC values of 36 reported. The second batch of material was IN718 sample coupons of 50 x 3 x 25 mm produced using selective laser melting (SLM). The samples were built up with the long side axis on the build plate by a commercial supplier

of additive material in the UK. Hardness measurements were made on this material and were found to have HRC values of 44. The samples were tested in the as-manufactured condition without any subsequent heat treatments. Additional testing is to be conducted on heat treated material at a later date.

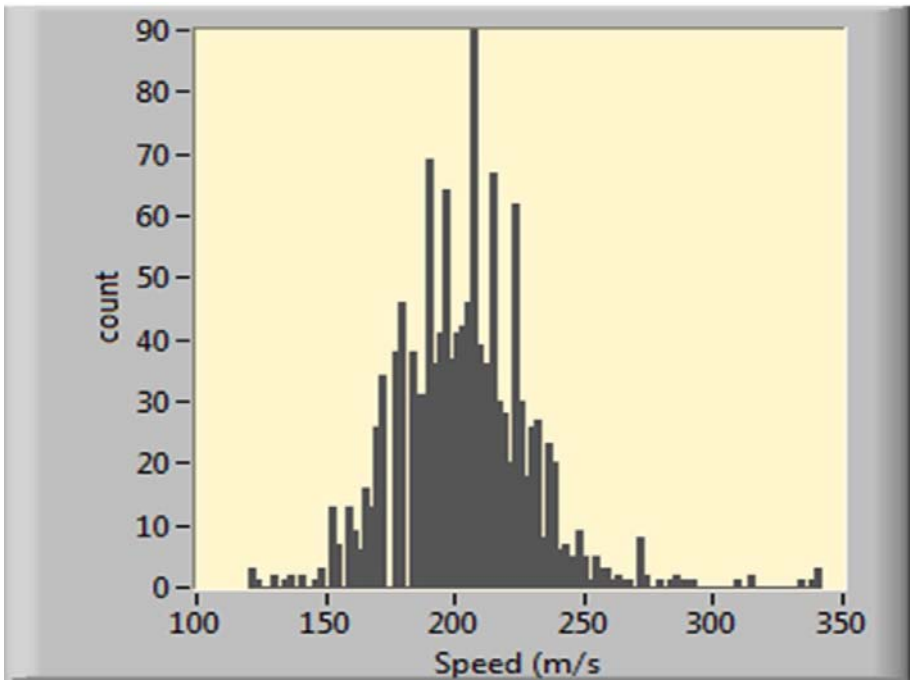

Figure 9 Velocity distribution for the Saftigrit White230-mesh alumina at a temperature of 700 °C within the NPL HTSPE test apparatus.

Table 1 Material compositions.

Material	Materials Composition, wt%												
	Ni	Cr	Nb	Mo	Ti	Al	Co	Cu	C	Si, Mn	P, S	B	Fe
Wrought IN718	54.6	18.7	5.07	3.01	0.88	0.46	0.03	0.05	0.021	0.11	<0.01	<0.005	Bal
SLM IN718*	50-55	17-21	4.75-5.5	2.8-3.3	0.65-1.15	0.20-0.80	<1.0	<0.3	<0.08	<0.35	<0.015	<0.006	Bal

* Nominal composition

RESULTS

The density of the two materials was calculated based on the mass of the samples and their dimensions, some uncertainty is expected due to the roughness of the SLM IN718 surfaces. The density of the wrought material was calculated to be 8.15 gcm^{-3} and the density of the SLM IN718 was 8.07 gcm^{-3}, equating to a difference of less than 1%.

Figure 10 shows an image of the eroded samples tested at 20, 400 and 500 °C, the erosion scar can be clearly observed with a track extending on the right-hand side of the scar. This track is caused by the 'parking' of the

nozzle during the erosion test which was performed with the powder flowing to ensure a consistent feed rate during the exposure.

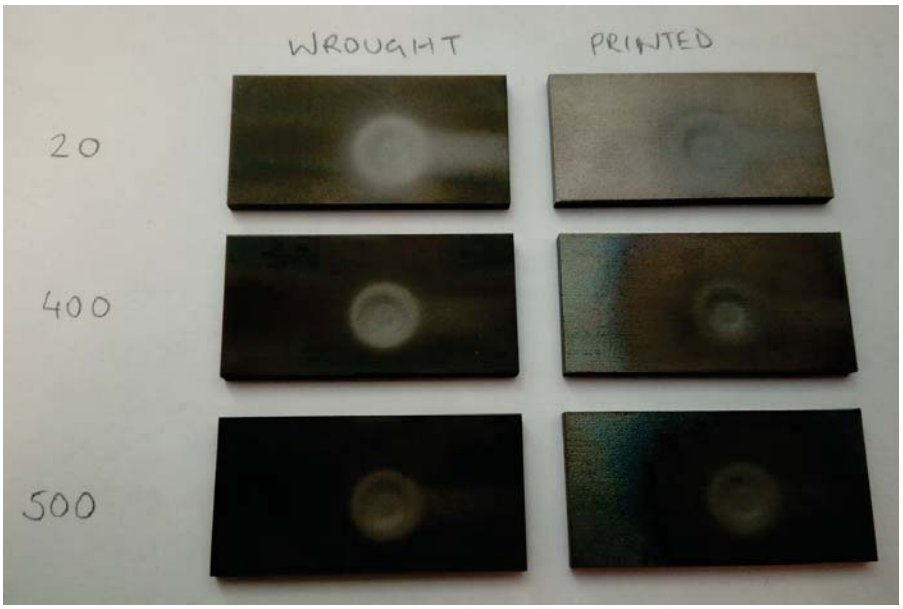

Figure 10 Photo of the six samples HTSPE tested.

During the test, images were generated to be used to construct depth maps. The resultant depth maps are presented in Figure 11, note the different scale for each set of images. Figure 11 clearly shows that, as one might expect, as the temperature increased so the depth of erosion also increased. The first maps in Figure 11a and 11c did not produce usable results due to insufficient laser line contrast caused by the surface contrast and scattering of the laser, changing the camera aperture would have adjusted for this but since this was only the first exposure of the flat surface these changes were deemed unnecessary.

Figures 12-14 show the volume loss as a function of erodent mass impinging on the surface at room temperature, 400 °C and 500 °C for both batches of material. These figures also compare the final value of volume of material loss from the *in situ* laser scanning measurements compared with the volume calculated from the *ex situ* mass change. These figures show that the *in situ* laser scanning measurements made at both room temperature and at elevated temperature are in very good agreement to the *ex situ* mass change / volume change measurements made at room temperature at the end of the test. In both the wrought and SLM IN718 the amount of material loss was found to increase with increasing temperature, plateauing at elevated temperature, and in both cases the amount of material loss was virtually the same for both sets of samples as shown in Table 2. The erosion rates, shown in Figure 15, were found to increase from 0.148 mm^{-3}/g erodent and 0.16 mm^{-3}/g erodent for the wrought and SLM IN718 to 0.355 and 0.361 mm^{-3}/g erodent at 500 °C respectively.

Table 2 Volume of material removed after 50g of erodent impinging on the sample surface.

HTSPE Temperature	Material loss, mm^{-3} (mass-based values shown in bracket)	
	Wrought IN718	SLM IN718
Room Temperature	-8.23 (-8.47)	-8.76 (-8.98)
400 °C	-17.34 (-17.94)	-17.49 (-18.10)
500 °C	-17.36 (-18.37)	-20.27 (-21.01)*

* value at 60g of erodent

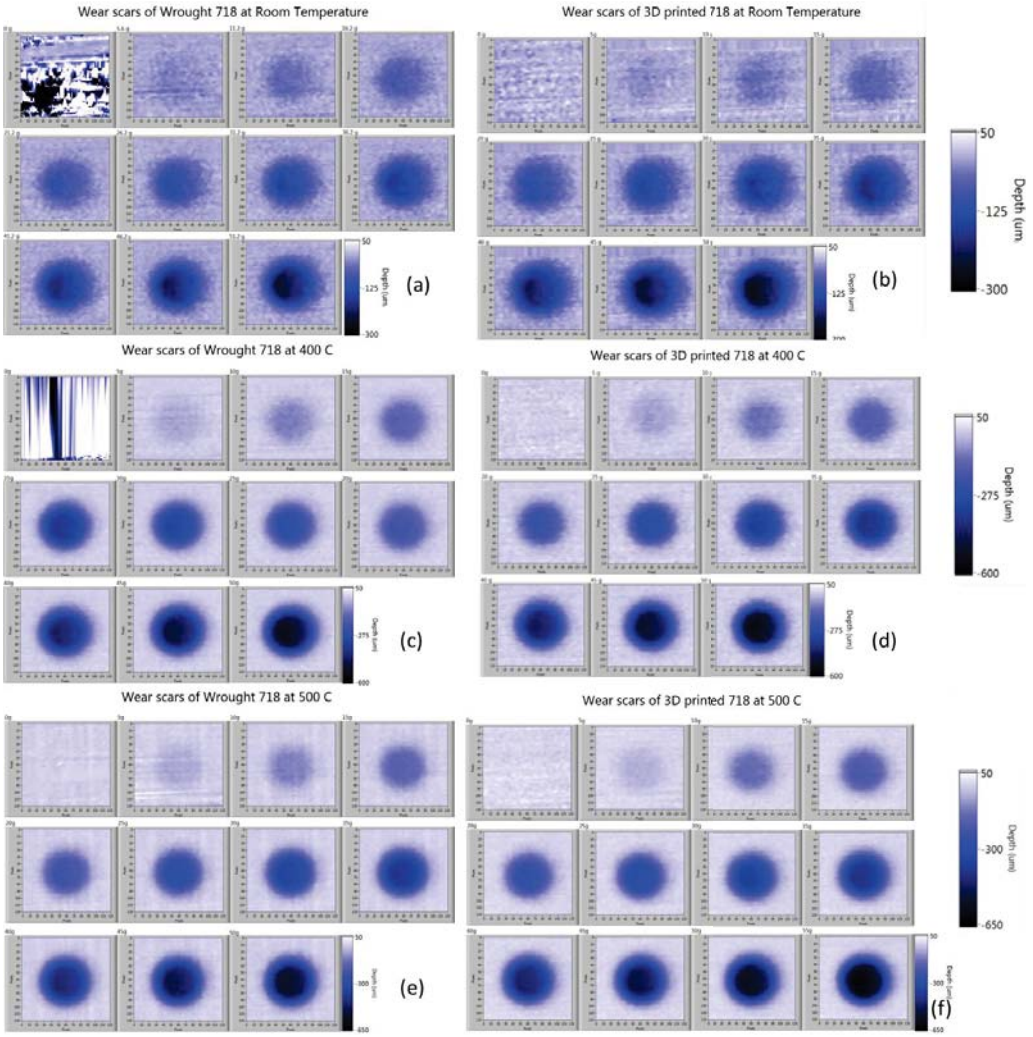

Figure 11 Depth maps for the wrought IN718 (a, c and e) and SLM IN718 (b, d and f) measured during the HTSPE tests at 20 °C (a and b), 400 °C (c and d) and 500 °C (e and f).

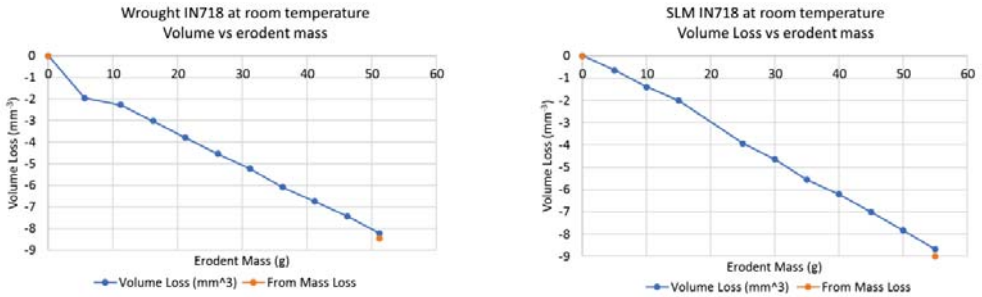

Figure 12 Volume loss as a function of erodent mass for wrought and SLM IN718 at room temperature.

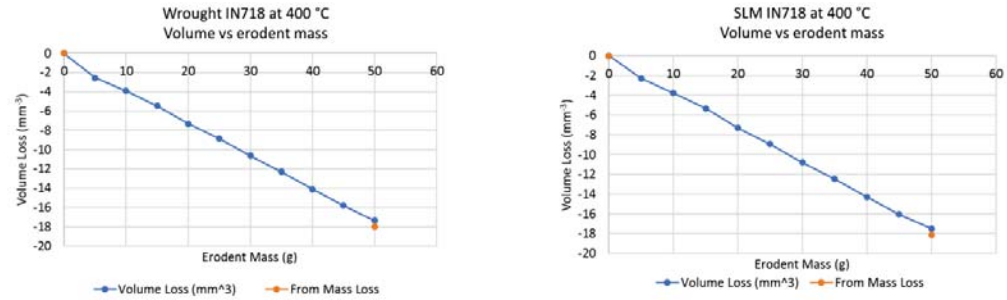

Figure 13 Volume loss as a function of erodent mass for wrought and SLM IN718 at 400 °C.

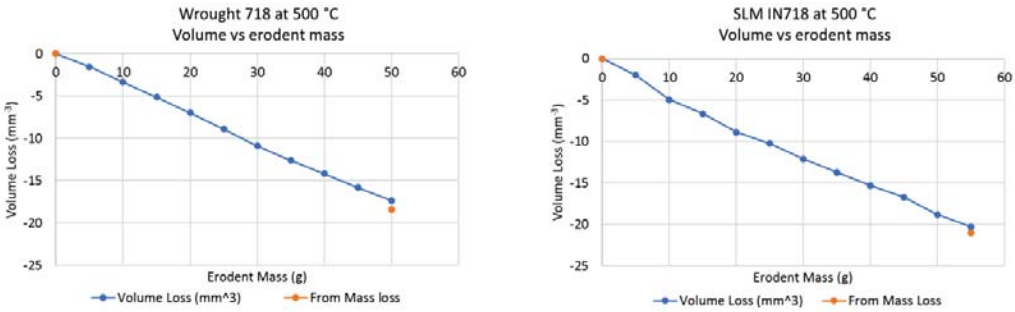

Figure 14 Volume loss as a function of erodent mass for wrought and SLM IN718 at 500 °C.

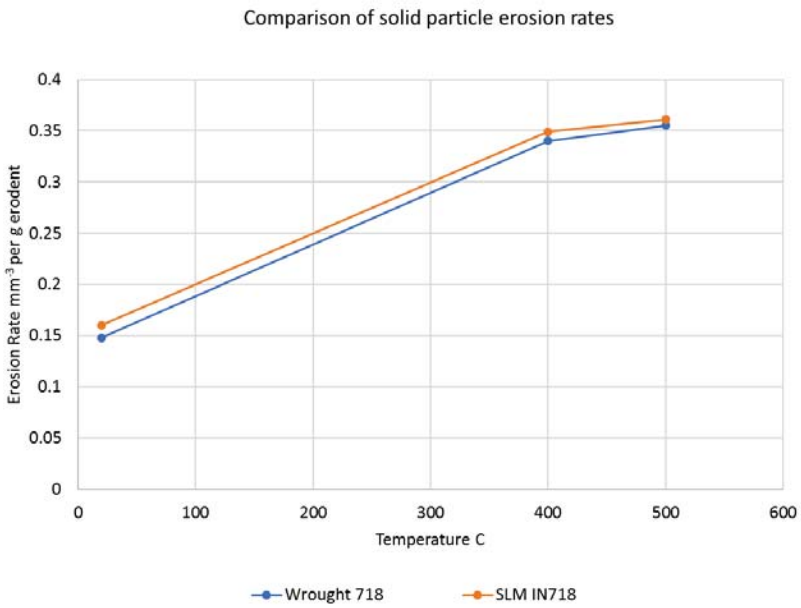

Figure 15 Comparison of the erosion rate for the wrought and SLM IN718 as a function of temperature.

CONCLUSIONS AND FURTHER WORK

- *In situ* measurements of the volume of material eroded during HTSPE tests in the NPL HTSPE apparatus have been successfully made at room temperature and at elevated temperature using the NPL laser triangulation scanner.
- Using this approach enables a full HTSPE test to be conducted in a matter of hours and avoids the introduction of errors caused by cooling of the sample, removal from the equipment and weighting at set periods to generate erosion curves.
- Comparison with measurements made using the mass change of the samples at the end of the test has shown that the *in situ* volume measurements are in good agreement thereby validating the measurements.
- The HTSPE erosion rate of wrought and SLM IN718 has been measured at room temperature and at 400 and 500 °C. In all cases the erosion rate was found to be the same, within the realms of experimental error, between the two material batches. This suggests that the as produced additively manufactured material has comparative erosion resistant (under these conditions) to the conventionally cast, forged and heat treated IN718.

- Further work is required to compare the two microstructures and to measure the Rockwell hardness of the wrought alloy, rather than using the certificated values, to determine any significant differences. In addition, it would be interesting to vary the impingement angle of the erodent to examine the influence of force made tangential to the 'printing' direction as opposed to perpendicular, as was the case reported here.

ACKNOWLEDGEMENTS

The authors wish to thank the UK Department for Business, Energy and Industrial Strategy for their support and funding through the National Measurement System.

REFERENCES

[1] M. J. Neale and M. G. Gee, Guide to Wear Problems and Testing for Industry, Professional Engineering Publishers, 2000.

[2] "ASTM G211 - Standard test method for conducting elevated temperature erosion tests by solid particle impingement using gas jets," ASTM, 2014.

[3] A. T. Fry, M. G. Gee, U. Neuschaefer-Rube, M. Bartscher, D. Spaltman, M. Woydt, S. Radek, J. Nicholls and T. W. Rose, "Metology to enable high-temperature erosion testing - a new European initiative," in *Advances in Materials Technology for Fossil Power Plants, Proceedings from the Seventh International Conference*, Waikola, HAwaii, 2013.

[4] N. A. S. Smith, A. T. Fry, L. E. Crocker, F. Cernuschi and L. Lorenzoni, "Design and optimisation of the nozzle of an innovative high temperature solid particulate erosion testing system using finite element modelling," *Applied Mathematics and Computation,* vol. 301, pp. 60-69, 2017.

[5] A. T. Fry, P. Lovelock, N. Smith, M. Gee and A. J. Gant, "An innovative high temperature solid particulate erosion testing system," *Wear,* vol. 376, pp. 458-467, 2017.

[6] A. T. Fry, D. Gorman, L. E. Crocker, M. G. Gee, A. Gant, J. Nicholls, T. Rose, F. Cernuschi, L. Lorenzoni and C. Guardamagno, "Influence of apparatus design and test methods on the high temperature solid particle erosion of nimonic 80A," in *Proceedings of the 8th International Conference on Advances in Materials Technology for Fossil Power Plants*, Algarve, Portugal, 2017.

[7] J. Nunn, M. Gee, L. Orkney and T. Fry, "In situ remote hot erosion scar measurement," *Wear,* Vols. 380-381, pp. 217-227, 2017.

[8] R. G. Dorsch, G. Hausler and J. M. Hermann, "Laser triangulation - fundamental uncertainty in distance measurement," *Appl Optics,* vol. 33, pp. 1307-1314, 1994.